CODEN IEJMAT *Internet Electronic Journal of Molecular Design* **2005**, *4*, 316–328 ISSN 1538–6414
BioChem Press http://www.biochempress.com

Inter*net* Electronic Journal of
Molecular Design

May 2005, Volume 4, Number 5, Pages 316–328

Editor: Ovidiu Ivanciuc

Computational Studies of 1*T* and 2*H* TaS_2 in Crystalline and Nanotubular Forms: Structural and Electronic Properties

Andrew N. Enyashin, Igor R. Shein, Nadezhda I. Medvedeva, and Alexander L. Ivanovskii

Institute of Solid State Chemistry, Ural Branch of the Russian Academy of Sciences, Ekaterinburg, 620219, Russia

Received: January 21, 2005; Revised: March 11, 2005; Accepted: March 15, 2005; Published: May 31, 2005

Citation of the article:
A. N. Enyashin, I. R. Shein, N. I. Medvedeva, and A. L. Ivanovskii, Computational Studies of 1*T* and 2*H* TaS_2 in Crystalline and Nanotubular Forms: Structural and Electronic Properties, *Internet Electron. J. Mol. Des.* **2005**, *4*, 316–328, http://www.biochempress.com.

Inter*net* Electronic Journal of Molecular Design

BioChem Press
http://www.biochempress.com

Computational Studies of 1*T* and 2*H* TaS_2 in Crystalline and Nanotubular Forms: Structural and Electronic Properties

Andrew N. Enyashin,* Igor R. Shein, Nadezhda I. Medvedeva, and Alexander L. Ivanovskii

Institute of Solid State Chemistry, Ural Branch of the Russian Academy of Sciences, Ekaterinburg, 620219, Russia

Received: January 21, 2005; Revised: March 11, 2005; Accepted: March 15, 2005; Published: May 31, 2005

Internet Electron. J. Mol. Des. **2005**, *4* (5), 316–328

Abstract

Motivation. Since the discovery of carbon nanotubes in 1991, inorganic nanotubes (NTs) have received much attention. The layered chalcogenides, having structures analogous to graphite, are known to be unstable toward bending and show high propensity to form curved structures. Recently, apart from carbon nanotubes, nanotubes of the layered *d*–metal disulfides (MS_2, M = Mo, W, Nb, Ta, Ti, Zr) have been synthesized. However the information on the structural and electronic properties of curved nanostructures based on tantalum disulfide is lacking to date. On the other hand, the study of TaS_2 bulk materials has been actively pursued during the last years owing their interesting properties and potential applications. One of the most important and intriguing problem that attracts the attention of researchers is the modification of properties of inorganic systems going from bulk to nanoscale state. In the present paper the electronic band structure of 1*T* and 2*H* polytypes of layered tantalum disulfide in crystalline and nanotubular forms has been studied by means of band structure approaches. For the first time we discuss the changes in electronic properties of TaS_2 nanotubes depending from the atomic arrangement in tube walls (octahedral or trigonal prismatic) and from the tube diameters and geometry (*zigzag* or *armchair*–like).

Method. The electronic band structures, densities of states, electron density maps, bonding indices – crystal orbital overlap populations and total band energies of 1*T* and 2*H* polytypes of TaS_2 bulk and nanotubes have been obtained using the *ab initio* full–potential linear muffin tin orbitals (FPLMTO) and the semi–empirical tight–binding EHT band structure approaches.

Results. The energy bands for 1*T* and 2*H* polytypes of crystalline TaS_2 are obtained; using of the total energy calculations, we found that there is a gain in energy of 0.231 eV/formula unit for 2*H* structure, reflecting the fact that the ideal 1*T* phase is unstable at low temperatures. The DOS at the Fermi energy $N(E_F)$ is controlled by the overlap between the S *p* and Ta *d* states. This overlap results in a metallic state for TaS_2. The DOS curves of 2*H* and 1*T* polytypes obtained by the semi–empirical EHT calculations are in reasonable agreement with *ab initio* FLMTO data. The atomic models of 1*T* and 2*H* TaS_2 nanotubes have been constructed. The electronic structure and bond indices of nanotubes have been calculated and analyzed as a function of the tubes diameters (D) in the *armchair*– and *zigzag*–like forms. Within the range of diameters examined, the *zigzag* configurations of 1*T* and 2*H* like tubes appear to be the most stable than *armchair* configurations. All NTs are metallic–like and their electronic spectra are similar to the DOS of the corresponding planar layers. The Fermi level is located in the region of the non–bonding Ta *d* band. For the *armchair*–like 2*H* TaS_2 NTs there is a pronounced DOS peak at the Fermi level. Since the this sharp DOS peak for such NTs is half–filled with high $N(E_F)$, one would expect that the some 2*H* TaS_2 NTs may be superconducting, as it has been obtained recently for $NbSe_2$ nanotubes

* Correspondence author; fax: +7–343–374449; E–mail: Enyashin@ihim.uran.ru.

(2003).

Conclusions. The electronic properties and chemical bonding of 2*H* and 1*T* polytypes of layered tantalum disulfide in crystalline and nanotubular forms have been studied with the *ab initio* FPLMTO and the semi–empirical tight–binding EHT approaches. We show that both *zigzag*– and *armchair*–like nanotubes are metallic–like, and the tube stability trends to vanish for very small NT diameters. *Zigzag*–like nanotubes were found to be more stable. It was established that Ta–S covalent bonds are the strongest interactions in TaS_2 bulk and NTs, whereas Ta–Ta bonds are much weaker.

Keywords. TaS_2; 1*T* and 2*H* polytypes; nanotube; band structure; chemical bonding; computer simulation.

1 INTRODUCTION

In the solid state chemistry and material science one of the most important and intriguing problem that attracts the attention of researchers is the modification of properties of inorganic systems going from bulk to nanoscale state. The discovery of carbon nanotubes [1] having unique structural, mechanical and electronic properties, and wide prospects of their application (including nanometer–sized semiconductor devices, sensors, field emission displays, energy storage and energy conversion devices, hydrogen storage materials etc, see [2–5]) paved the way to the discovery of nanotubular forms of other inorganic materials.

Nanotubes (NTs) of the layered molybdenum disulfide, MoS_2, became the first inorganic NTs [1], synthesized soon after the discovery of carbon NTs [6]. For the last years other *d*–metal dichalcogenides MX_2 (M = Mo, Ta, Zr, Hf, Nb; X = S, Se, Te) nanotubes, nanofibers and also fullerene–like molecules have been reported, see reviews [2–5,7].

As well as other layered compounds, TaS_2 can be regarded as quasi two–dimensional (2*D*) S–Ta–S sandwiches with strong and primarily covalent intralayer bonding, while the interlayer bonding is weak and of Van der Waals type. TaS_2 can form more than one stacking polytype. The two most abundant polytypes of TaS_2 are the 1*T* and 2*H* with D^3_{3d} ($P3m1$) and D^4_{6h} ($P6_3/mmc$) space groups, respectively, where each tantalum is coordinated by six sulfur atoms in either an octahedral (1*T*) or trigonal prismatic (2*H*) arrangement. 2*H* polytype is stable at room temperature. The undistorted 1*T* phase exists for a very small temperature range above 550 K. Upon cooling, it shows a charge–density waves (CDW), manifested in periodic lattice distortions.

Tantalum disulfide is of strong interest for a long time because of their unique physical properties. Particularly, for the 1*T* octahedrally coordinated polytype the Fermi surface is very simple and two–dimensional one, with large near–parallel walls. Such situation is known theoretically to favor the formation of charge and spin–density waves. Thus 1*T*–TaS_2 is a prototype for such layered materials with a rich phase diagram of commensurate and incommensurate CDW's, see [8–10]. 1*T* and 2*H* polytypes may be regarded as the fundamental structures on which the other more complex mixed coordination polytypes of TaS_2 (3*R*, 4*H*, 6*R* etc) are based. These

2*D*–like structures have been widely used for intercalation and a wide family of TaS_2 – based *misfit* compounds was obtained [11,12].

Recently the nanotubes of layered tantalum disulfide have been successfully synthesized [13–15]. The crystalline tantalum trisulfide was used as an initial material, and the nanotubes were obtained at ~ 1000 °C by the simple hydrogen reduction reaction: $TaS_3 + H_2 \rightarrow TaS_2 + H_2S$. The TEM images shows a TaS_2 nanotubes with a hollow core of diameter about 20–40 nm and organized layers of the disulfide along the tube walls. Some of the tubes are closed with a nearly flat rectangular tips. Electron diffraction pattern of the NTs was similar to that of bulk TaS_2 (with ~ 3% expansion along the *c*–axis); the chemical composition of the nanotubes is close to Ta:S ratio of 1:2. The EDX analysis and the XRD confirmed the product to be 2*H* TaS_2.

In the present paper the electronic properties of layered 2*H* and 1*T* polytypes of TaS_2 in crystalline and nanotubular forms are calculated by the full–potential linear *muffin–tin* method (FLMTO) method within the local density approximation (LDA) as well as the semi–empirical tight–binding Extended Hückel (EHT) approaches. The first method (FLMTO) provides *ab initio* band structures, the density of states (DOS) and the valence charge densities, while the second one was used for chemical bonding analysis by means of a crystal orbital overlap populations (COOP).

We have also calculated the band structure of TaS_2 NTs and discussed the influence of the tube geometry (*zigzag* – or *armchair*–like) and the type of local coordination of the metal: octahedral (1*T*) *versus* trigonal–prismatic (2*H*) on their electronic properties.

2 MODELS AND METHODS OF CALCULATIONS

1*T* TaS_2 crystallizes in the CdI_2–type structure (space group *P*3*m*1) with the lattice parameters *a* = 0.3365, *c* = 0.5853 nm [16] and one formula per unit cell (Z = 1). One Ta atom is at 1*a* (0,0,0) and two S atoms are at 2*d* (⅓,⅔,z) and (⅔,⅓,–z), z = 0.257. The hexagonal TaS_2 consists of triple (S–Ta–S) layers, where a Ta sheet is sandwiched between two sulfur sheets. The metal atoms are surrounded by six anions with approximately octahedral spheres. Each sulfur atom is coordinated to three tantalum atoms with a trigonal pyramidal geometry.

For 2*H* TaS_2 the coordination of the tantalum by the sulfur is trigonal prismatic, there are two layers per unit cells (Z = 2) staked in hexagonal symmetry, where the Ta and S atoms occupy the positions 2*b* and 4*f* (with z = 1/8), respectively. The individual S–Ta–S layers are displaced by ⅓ along the *a* and *b* directions resulting in a *AcA–BcB* stacking sequence along the *c* axis. The lattice parameters are *a* =0.3316, *c* =1.2070 nm [16].

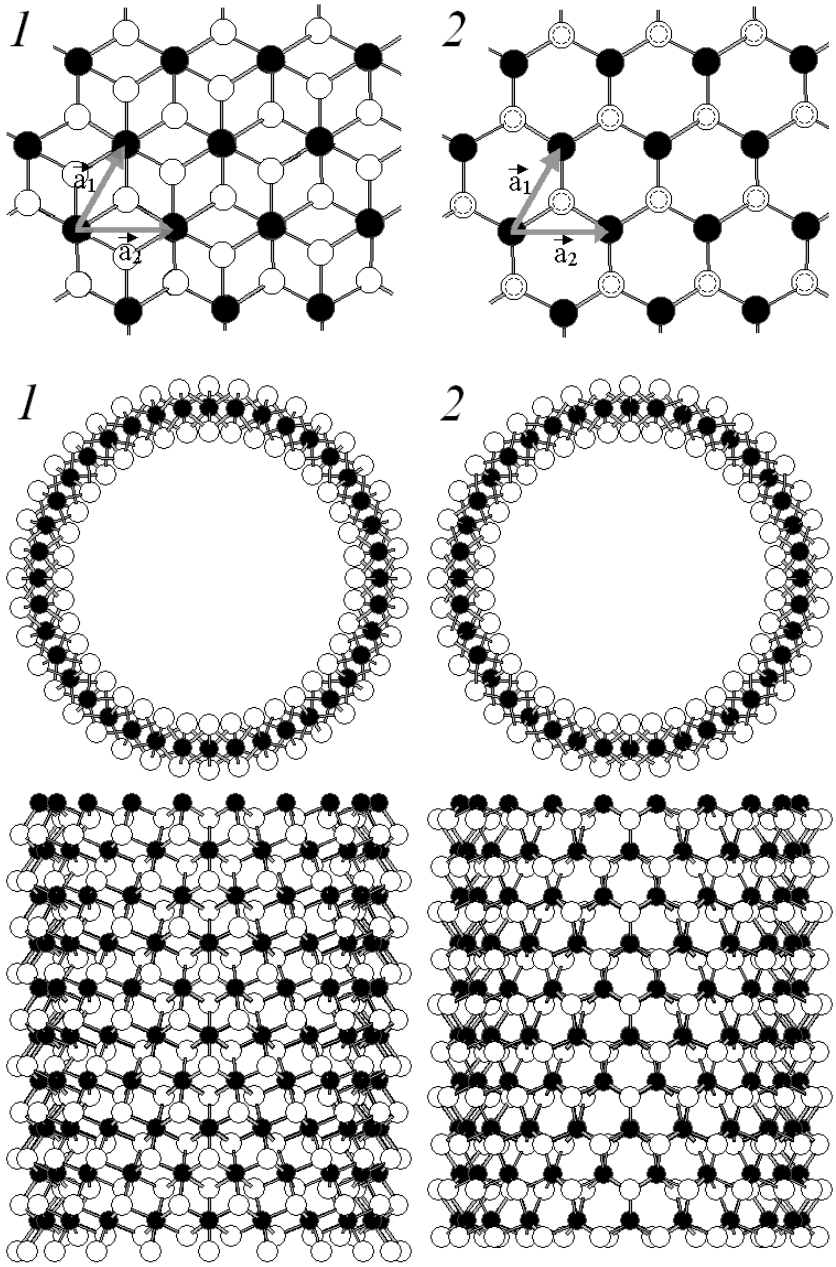

Figure 1. Atomic structures of *1* – 1*T* and *2* – 2*H* TaS_2 monolayers; ○ – sulfur and ● – tantalum atoms; $\boldsymbol{a_1}$ and $\boldsymbol{a_2}$ – basis vectors of the Ta plane sheets (upper panel). Lower panel: atomic structures of *zigzag* (20,0) NTs based on *1*– 1*T* and *2* – 2*H* TaS_2. Top views and views along the tube axis are shown.

The atomic models of TaS_2 infinite–long tubes were constructed by mapping the 1*T* and 2*H* S–Ta–S layers onto the surface of a tube. These "single–walled" tubes consist of three coaxial S–Ta–S cylinders, Figure 1. The geometry of TaS_2 tubes was described by the basis vectors $\boldsymbol{a_1}$ and $\boldsymbol{a_2}$, Figure 1. As in carbon [2,3] or other *d*–metal dichalcogenide tubes [17–22], three groups of 1*T* and 2*H*–like TaS_2 NTs can be obtained depending on the rolling direction $\boldsymbol{c} = n\boldsymbol{a_1}+m\boldsymbol{a_2}$: non–chiral *armchair* (n,n)–, *zigzag* (*n*,0)–, and chiral (*n*,*m*)–like nanotubes. We calculated the electronic structure of infinite–long (*n*,0) and (*n*,*n*) TaS_2 tubes as a function of *n* from 5 to 25. The geometrical

parameters of these tubes (namely the diameters of the "central" tantalum cylinders D(Ta) and the diameters of "inner" and "outer" sulfur cylinders $D(S^{in})$ and $D(S^{out})$) are listed in Table 1.

Table 1. The diameters (in nm) of atomic cylinders for 1*T* and 2*H* TaS_2 nanotubes

1*T*–TaS_2 NTs	$D(S^{in})$ [a]	$D(S^{out})$	D(Ta)	2*H*–TaS_2 NTs	$D(S^{in})$	$D(S^{out})$	D(Ta)
(5,0)	0.1339	0.7328	0.5357	(5,0)	0.1317	0.7205	0.5267
(10,0)	0.7375	1.3004	1.0714	(10,0)	0.7251	1.2785	1.0534
(15,0)	1.2941	1.8497	1.6071	(15,0)	1.2724	1.8187	1.5801
(20,0)	1.8399	2.3929	2.1428	(20,0)	1.8089	2.3527	2.1067
(25,0)	2.3814	2.9332	2.6784	(25,0)	2.3414	2.8839	2.6334
(5,5)	0.5575	1.1377	0.9278	(5,5)	0.5482	1.1186	0.9122
(10,10)	1.5363	2.0939	1.8557	(10,10)	1.5105	2.0587	1.8245
(15,15)	2.4798	3.0330	2.7835	(15,15)	2.4381	2.9820	2.7367
(20,20)	3.4152	3.9669	3.7114	(20,20)	3.3578	3.9002	3.6490
(25,25)	4.3475	4.8984	4.6392	(25,25)	4.2744	4.8161	4.5612

[a] Diameters: of the of "inner", "outer" sulfur and "central" tantalum cylinders, see Figure 1

Band structure calculations were performed by a scalar relativistic self–consistent FLMTO within the local density approximation (LDA) [23, 24] using codes from Ref. [25]. All *k*–space integrations were performed with the tetrahedron method using 32 *k* points within the Brillouin zone (BZ). The basis sets were consisted of 6*s*, 6*p* and 5*d* for Ta, and 3*s*, 3*p* and 3*d* orbitals for sulfur. To investigate the chemical bonding, the COOP values were calculated within the tight–binding Extended Hückel (EHT) method [26]. This method is used also for the calculations of the electronic band structure, the DOSs and the total energies (E_{tot}) for 1*T* and 2*H* TaS_2 tubular forms.

3 RESULTS AND DISCUSSION

The energy bands for 1*T* and 2*H* polytypes of crystalline TaS_2 along the high–symmetry directions in the BZ are shown in Figure 2. In Table 2 we summarize our numerical results for the band structure parameters. First of all, using of the total energy calculations, we found that there is a gain in energy of 0.231 eV/formula unit for 2*H* structure, reflecting the fact that the ideal 1*T* phase is unstable at low temperatures.

For 2*H* phase the lowest four bands (around – 12 eV, they are not shown in Figure 2) originate from S 3*s* states; bands ranging from – 6.2 eV to E_F are the sulfur 3*p* bands with an appreciable amount of Ta 5*d* states. The two half–filled bands crossed by the Fermi level are Ta 5*d* bands with S 3*p* admixture. The Ta $5d_{xz,yz}$ states dominate in the S 3*p* region and form the covalent σ bonds with the fully occupied S $3p_{x,y}$ states. On the contrary, two high energy Ta $5d_{z^2-1,xy}$ bands are separated from the S 3*p* bands, and only S $3p_z$ band brings the contribution in the DOS at the Fermi level.

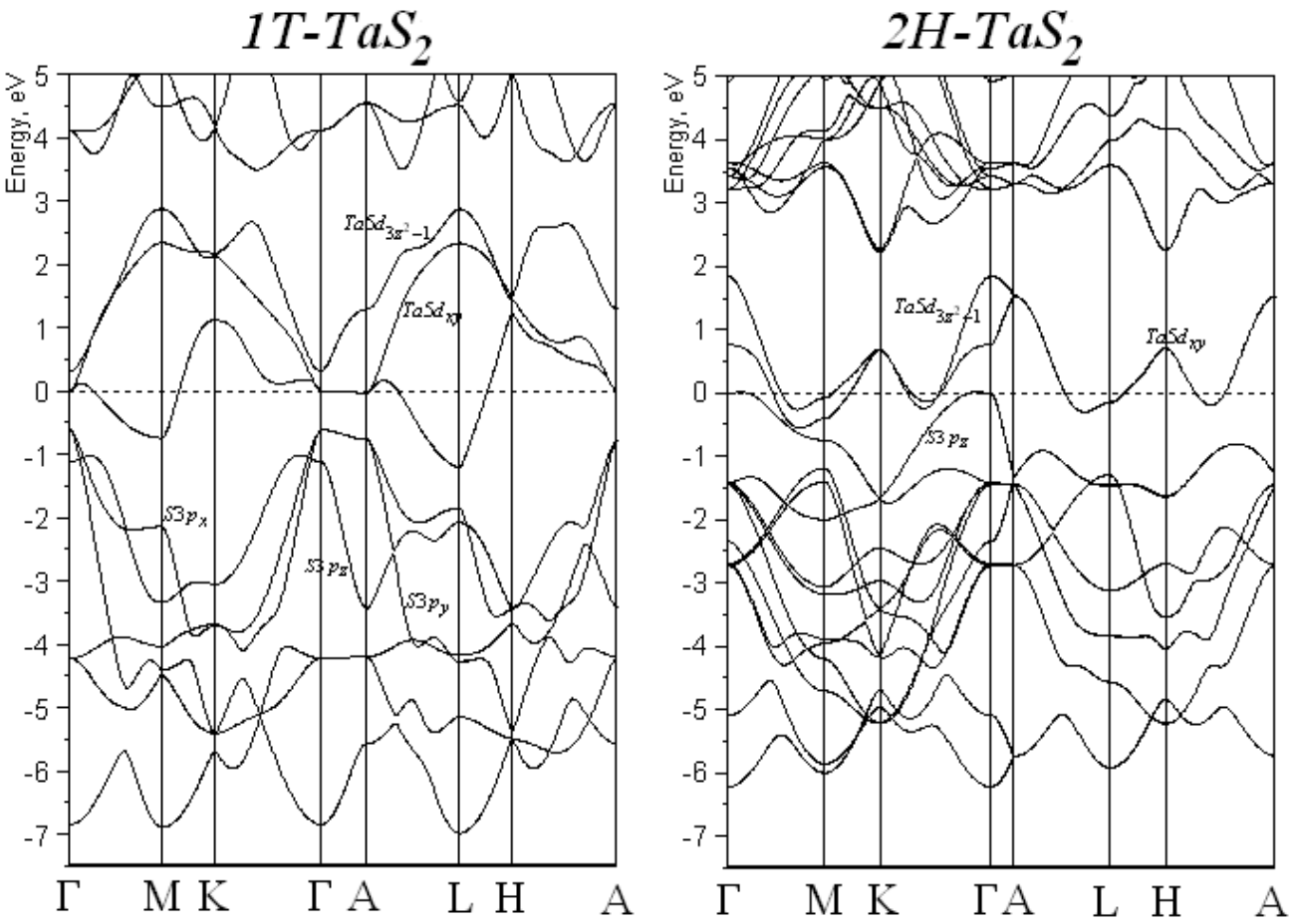

Figure 2. Electronic bands of 1*T* and 2*H* polytypes of tantalum disulfide along some symmetry axes according to FPLMTO calculations. The main contributions of Ta and S states are indicated near E_F.

Table 2. Density of states at the Fermi level (DOS, states/eV, FPLMTO data) and crystal orbital overlap populations (COOPs, e/bond) for 1*T* and 2*H* TaS_2

Polytype/DOSs	Ta*6s*	Ta*6p*	Ta*5d*	Ta*4f*	S*3s*	S*3p*	S*3d*
1*T*–TaS_2	0.020	0.010	0.925	0.007	0.021	0.353	0.090
2*H*–TaS_2	0.013	0.050	1.430	0.013	0.029	0.678	0.102

Polytype/COOPs	Ta–S	Ta–Ta	S–S
1*T*–TaS_2	0.225	0.024	0.0
2*H*–TaS_2	0.219	0.041	0.0

The valence band (VB) for 1*T* TaS_2 includes six occupied bands and has a width of about 13.5 eV. The topmost partially occupied band located on tantalum atoms along Γ–M–K–Γ is strongly localized in plane and delocalized out of plane (Γ–A). Comparing the band structures of 1*T* and 2*H* polytypes, we note that Ta *d* manifold splitting as well as *p–d* hybridization are larger in 1*T* TaS_2 (octahedral) that reflects the separation of non–bonding *d* and mixed *p–d* bands, Figure 2.

The density of states (DOSs) obtained from our FPLMTO calculations are shown in Figure 3. For 1*T* polytype the sharp peak around –12.9 eV is mainly due to the quasi–core S 3*s* states, the

peaks around –5.5 and –2.2 eV are due to S *p* states, and the middle peak –3.9 eV peak is made of the comparable contributions of Ta *d* and sulfur *p* states. Within the conductivity band, the peaks at 0.6, 2.3, and 2.7 eV have mainly Ta *d* character. The DOS at the Fermi energy $N(E_F)$ is controlled by the overlap between the S *p* and Ta *d* states. This overlap results in a metallic state with a DOS at the E_F ($N(E_F)$) of 1.42 states/(eV cell). The main contributions in $N(E_F)$ arise from Ta *d* (65%) and S *p* (25%) states.

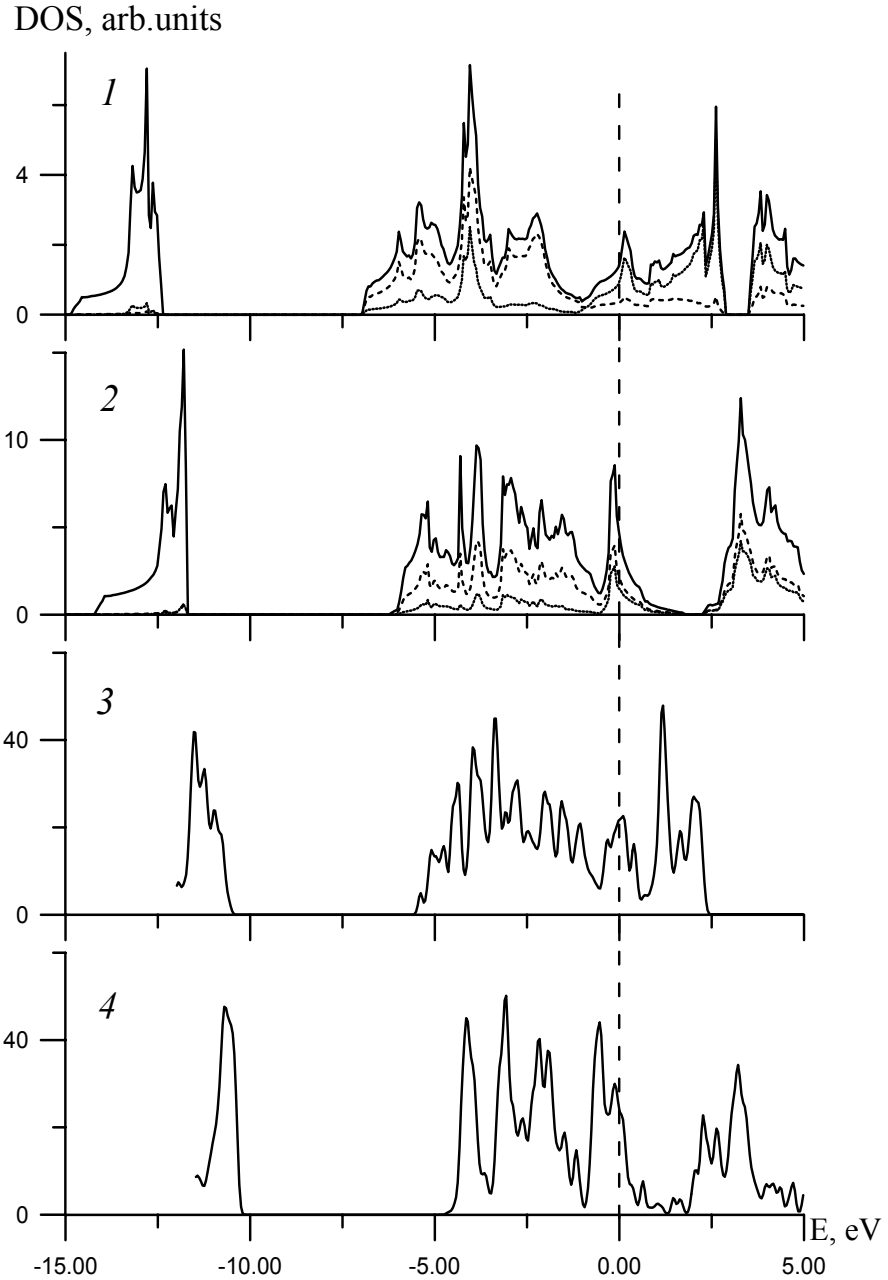

Figure 3. The total densities of states (TDOSs) for crystalline 1*T*– (*1*,*3*) and 2*H*– (*2*,*4*) TaS_2 according to FPLMTO (*1*,*2*) and semi–empirical EHT (*3*,*4*) calculations. For 1*T*– (1) and 2*H*– (2) polytypes the Ta5*d* (*solid lines*) and sulfur 3*p* (*dotted lines*) states are given. Vertical lines denote the Fermi level.

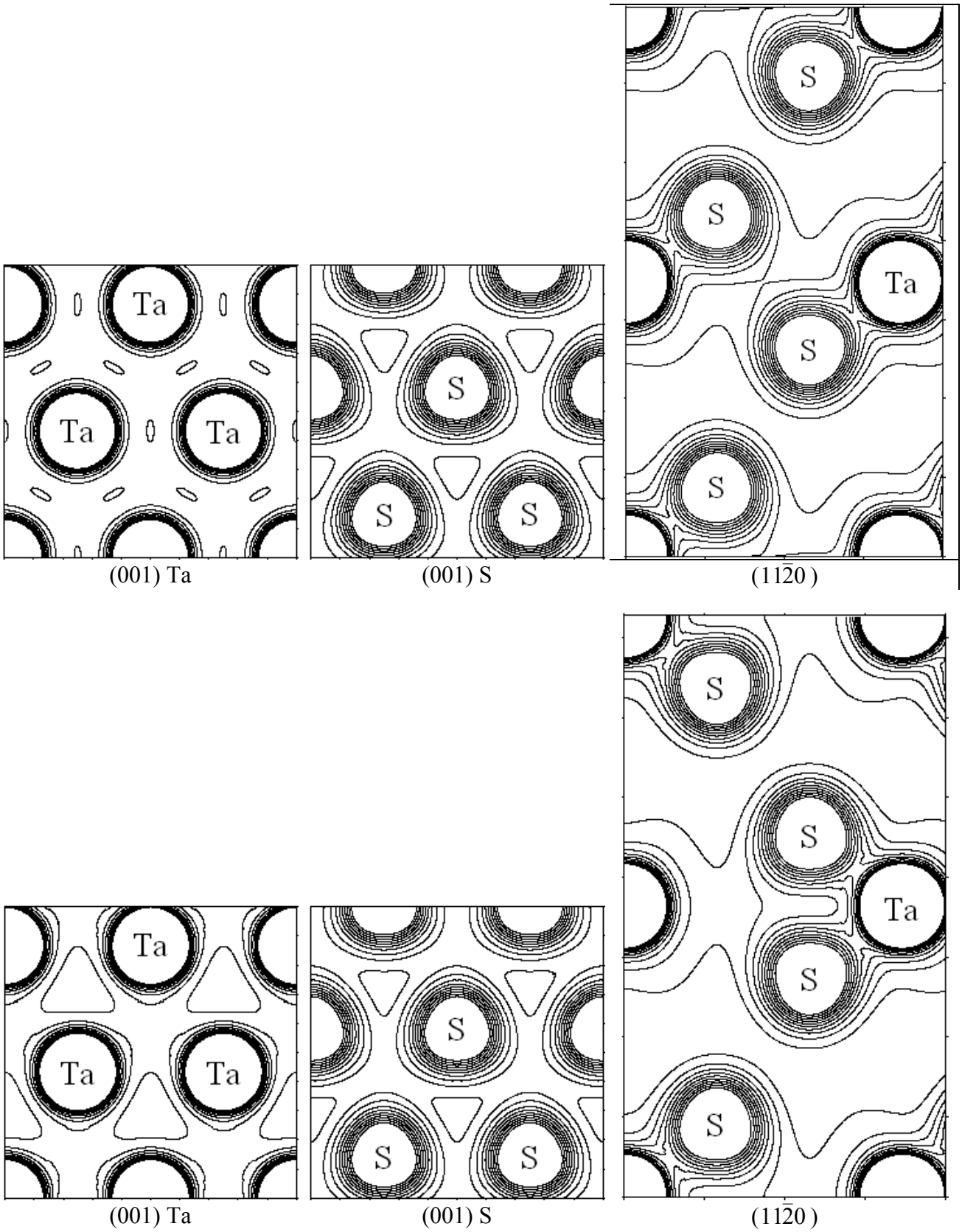

Figure 4. Valence charge densities in Ta (001), S (001) and (11$\bar{2}$0) sections of 1*T*– (upper panel) and 2*H*–TaS_2 according to FPLMTO calculations. The successive contour lines differ by 0.1 e/Å^3.

The calculated DOSs for 1*T* polytype showed some differences as compared with DOS for the 2*H* phase. For 2*H* phase the peak of the quasi–core S 3*s* states is around –11.9 eV. The DOSs peaks (in the region of hybridized *p–d* bands: from –6.1 eV to E_F) are less pronounced than for 1*T* polytype. On the contrary, as it is seen from Figure 3, the DOS for 2*H* phase contains a sharp peak near –0.06 eV arising from the Ta *d*–like band, that is quasi–flat along Γ–A symmetry direction. The main contributions in $N(E_F)$ are given Ta *d* states (~61%) and S *p* (29%) states. The double peak composed of the S *p* – Ta *d* anti–bonding states located at ~ 3.1 – 4.0 eV is also observed in S *K–edge* XANES spectra [27]. The DOS curves of 2*H* and 1*T* polytypes obtained by the semi–empirical EHT calculations are in reasonable agreement with *ab initio* FLMTO data, Figure 3.

The electron density (ρ) maps at the (001) and $(11\bar{2}0)$ planes for 1*T* and 2*H* polytypes are shown in Figure 4. The density maps show a sharp asphericity of the ρ contours in the direction of the Ta–S bonds, indicating a strong covalent character of the Ta–S bonding. The ρ maps on the $(11\bar{2}0)$ planes also demonstrate an insignificant electron density accumulation in the interlayer region indicating the absence of covalent S–S bonding in interlayer direction. Electron density accumulation in the Ta interatomic region (tantalum (001) planes) is observed, indicating the Ta–Ta metallic–like bonds, which are weaker for 1*T* than for 2*H* polytype.

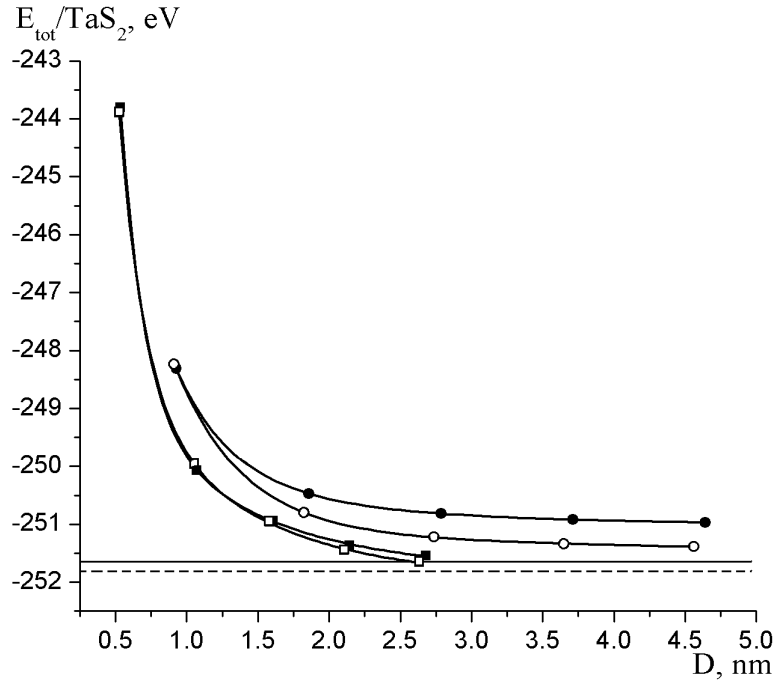

Figure 5. Total energies (E_{tot}, per TaS_2 unit) as a function of the: (○,□) 1*T*– and (●,■) 2*H*–TaS_2 NT diameters of the *armchair*– (○,●) and *zigzag*–like (□,■) configuration, according to EHT calculations. The energies of planar 1*T*– (solid line) and 2*H*–TaS_2 (dotted line) monolayers are also presented.

COOPs analysis (Table 2) reveals that two main types of Ta–S and Ta–Ta covalent bonds exist in both polytypes, whereas S–S bonding is practically absent (COOPs ~0). The Ta–S bonds are

much stronger, than Ta–Ta bonds. Our results indicate also an increase of Ta–S covalency (by 7 %) going from 2*H* to 1*T*. On the contrary, COOPs values of weak Ta–Ta bonds increase during 1*T*→2*H* transition. Let's note that COOPs values of all intra–layer atomic S–S bonds are close to zero, and inter–layer interaction is of the Van der Waals type.

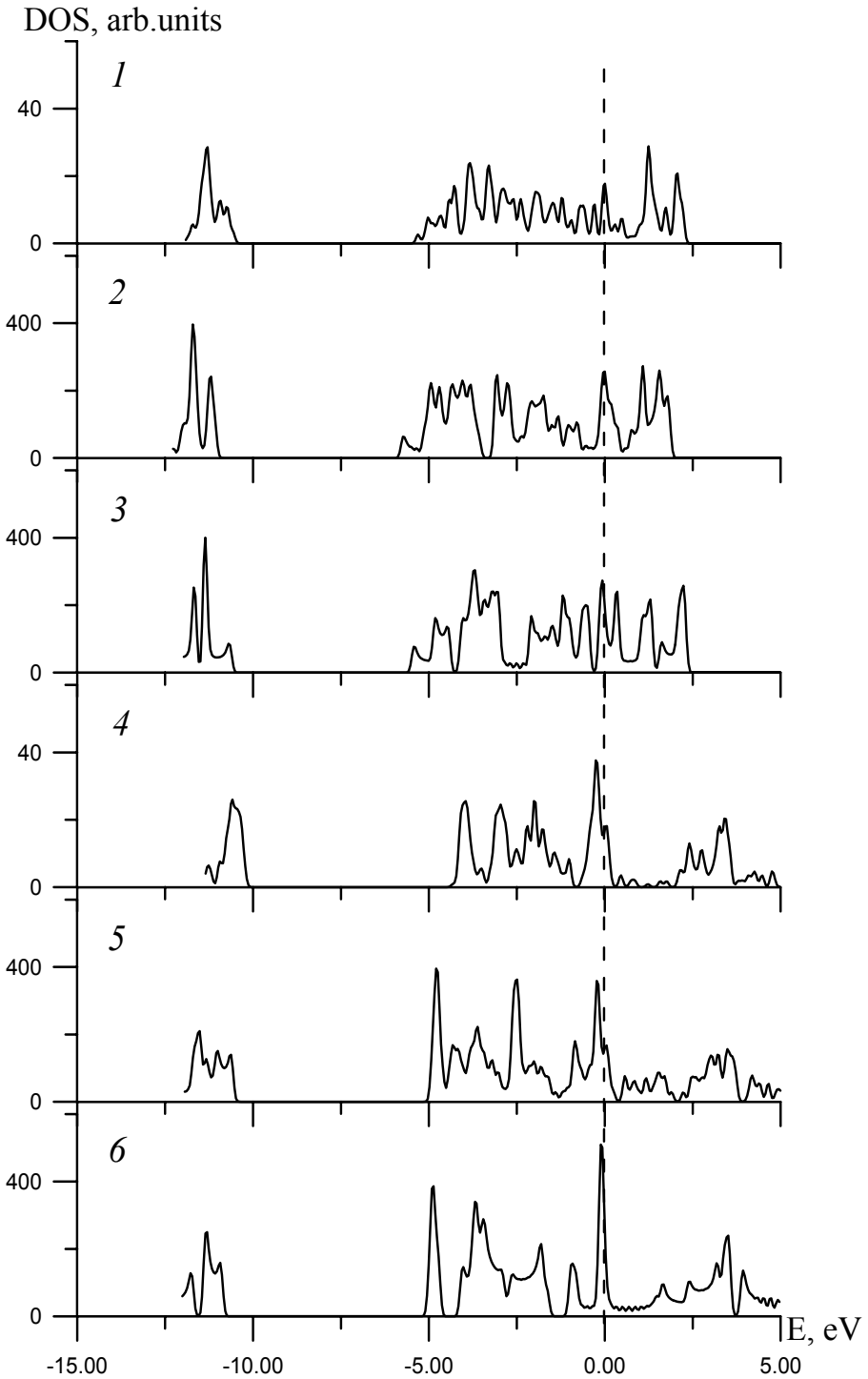

Figure 6. Total DOSs of: *1*, *4* – 1*T*–, 2*H*– TaS_2 monolayers, *2*, *5* – (25,0); *3*, *6* – (25,25) NTs of *2*, *3* – 1*T*–, and *5*, *6* – 2*H*–TaS_2, respectively, according to EHT calculations. Vertical lines denote the Fermi level.

Using atomic models, presented in section 2 and EHT technique, we have determined also the electronic properties and bonding indices of TaS_2 nanotubes based on the 1*T* and 2*H* polytypes. Our results are summarized in Table 3 and Figures 5, 6. Figure 5 shows the calculated values of E_{tot} (per TaS_2 unit) *versus* the diameters D of tantalum disulfide NT. These data indicate that, the stability of the tubes decreases rapidly ($\sim 1/D^2$), that reflects the increase in strain energies of planar TaS_2 stripes upon rolling up them into cylinders. When the diameter D increases the total energy of the tubes asymptotically tends to E_{tot} for the corresponding planar TaS_2 monolayers. An analogous dependence is typical for other disulfide NTs and was also obtained in earlier studies for MoS_2, WS_2, ZrS_2, NbS_2 and $NbSe_2$ NTs [20–23].

It is worth noting that, within the range of diameters examined, the *zigzag* configurations of 1*T* and 2*H* – like tubes appear to be the most stable than *armchair* configurations. In turn, the E_{tot} values for the *zigzag* 1*T* and 2*H* – like tubes are virtually the same, whereas among armchair–like the 1*T* NTs are the most stable. Obviously, the additional contribution to the stabilization of the TaS_2 tubular structures is made by the Van der Waals interaction between the walls of adjoining coaxial (S–Ta–S) cylinders giving rise predominately to multi–walled TaS_2 NTs of rather large diameters.

Let us consider the band structures of (*n*,*n*) and (*n*,0) TaS_2 NTs. As follows from our calculations, all 1*T* and 2*H* TaS_2 NTs are metallic–like and their electronic spectra are similar to the DOS of the corresponding planar layers, Figure 6. The Fermi level is located in the region of the non–bonding Ta *d* band. The main interesting differences in the electronic states of the *armchair*– and *zigzag*–like TaS_2 NTs are connected with the near–Fermi DOS shape. From Figure 6 it is seen that for the *armchair*–like 2*H* TaS_2 NTs there is a pronounced DOS peak at the Fermi level. Since the this sharp DOS peak for such NTs is half–filled with high $N(E_F)$, one would expect that the some 2*H* TaS_2 NTs may be superconducting, as it has been predicted for isoelectronic NbS_2 tubes [18] and were obtained recently for $NbSe_2$ nanotubes [28].

Table 3. The parameters of chemical bonding (COOPs, e) in 1*T* and 2*H* TaS_2 nanotubes

Nanotube	Ta–S^{in} (1) [a]	Ta–S^{in} (2)	Ta–S^{out} (1)	Ta–S^{out} (2)	Ta–Ta (1)	Ta–Ta (2)
1*T*–TaS_2 (25,25)	0.496	0.658	0.291	0.690	0.035	0.021
2*H*–TaS_2 (25,25)	0.517	0.619	0.316	0.658	0.049	0.023

[a] COOPs for bonds along (1) and across (2) relative to the NT axis

The strength of covalent bonds in the TaS_2 tubes can be discussed using the COOP values, Table 3. For all tubes the main bonds are Ta–S interactions, and the population of the Ta–Ta bonds is an order of magnitude smaller. As well as in crystalline TaS_2 phases, the covalent S–S interactions for

nanotubes are absent (COOPs < 0). There is anisotropy of Ta–S bonds, which depends on both their orientation (across or along) relative to the NT axis and the positions of S atoms belonging to inner or outer cylinders (Ta–S^{in}, Ta–S^{out} bonds, Table 2). For the considered NTs, the COOPs values of some Ta–S^{out} bonds are minimal. This suggests higher reactivity of the outer sulfur atoms and a possibility of their rearrangement with the formation atomic defects in the outer tube walls.

4 CONCLUSIONS

In summary, the electronic properties and chemical bonding of *2H* and *1T* polytypes of layered tantalum disulfide in crystalline and nanotubular forms have been studied with the *ab initio* full–potential linear muffin tin orbitals (FPLMTO) and the semi–empirical tight–binding EHT approaches. We show that both *zigzag*– and *armchair*–like nanotubes are metallic–like, and the tube stability trends to vanish for very small NT diameters. *Zigzag*–like nanotubes were found to be more stable. It was established that Ta–S covalent bonds are the strongest interactions in TaS_2 bulk and NTs, whereas Ta–Ta bonds are much weaker.

Acknowledgment

The author acknowledges financial support from the RFBR, grants 04–03–32111 and 04–03–96117 (Ural) and by the Russian Foundation for Scientific Schools, grant SS 829.2003.3.

5 REFERENCES

[1] S. Iijima, Helical microtubules of graphitic carbon, *Nature* (*London*) **1991**, *354*, 56–58.
[2] A. Zettl, Non–carbon nanotubes, *Adv*. *Mater*. **1996**, *8*, 443–445.
[3] R. Tenne, Inorganic Nanoclusters with Fullerene–Like Structure and Nanotubes, *Progr*. *Inorg*. *Chem*. **2001**, *50*, 269–315.
[4] A. L. Ivanovskii, Non–carbon nanotubes: synthesis and simulation, *Russ*. *Chem*. *Rev*. **2002**, *71*, 175–194.
[5] R. Tenne, Inorganic Nanotubes and Fullerene–Like Materials, *Chemistry – Europ*. *J*. **2002**, *8*, 5296–5304.
[6] R. Tenne, L. Margulis, M. Genut, G. Hodes, Polyhedral and cylindrical structures of tungsten disulphide, *Nature* (*London*) **1992**, *360*, 444–446.
[7] C. N. R. Rao, M. Nath, Inorganic Nanotubes, *Dalton Trans*. **2003**, *1*, 1–24.
[8] W. C. Tonjes, V. A. Greanya, R. Liu, C. G. Olson, P. Molinie, Charge–density–wave mechanism in the 2*H*–$NbSe_2$ family: Angle–resolved photoemission studies, *Phys*. *Rev*. *B* **2001**, *63*, 235101.
[9] K. Horiba, K. Ono, J. H. Oh, T. Kihara, S. Nakazono, M. Oshima, O. Shiino, H. W. Yeom, A. Kakizaki, Y. Aiura, Charge–density wave and three–dimensional Fermi surface in 1*T*–$TaSe_2$ studied by photoemission spectroscopy, *Phys*. *Rev*. *B* **2002**, *66*, 073106.
[10] Y. Aiura, H. Bando, R. Kitagawa, S. Maruyama, Y. Nishihara, K. Horiba, M. Oshima, O. Shiino, M. Nakatake, Electronic structure of layered 1*T*–$TaSe_2$ in commensurate charge–density–wave phase studied by angle–resolved photoemission spectroscopy, *Phys*. *Rev*. *B* **2003**, *68*, 073408.
[11] G. A. Wiegers, A. Meetsma, S. Van Smaalen, R.J. Haange, J. Wulff, T. Zeinstra, J. L. De Boer, S. Kuypers, G. Van Tendeloo, J. Van Landuyt, S. Amelinckx, A. Meer–Schaut, P. Rabu, J. Rouxel, Misfit layer compounds $(MS)_nTS_2$ (M = Sn, Pb, Bi, rare earth elements; T = Nb, Ta; N = 1.08 – 1.19), a new class of layer compounds, *Solid State Commun*. **1989**, *70*, 409–413.

[12] J. L. De Boer, A. Meetsma, Th. J. Zeinstra, R. J. Haange, G. A. Wiegers, Structures of the misfit layer compounds $(LaS)_{1.13}TaS_2$, $LaTaS_3$ and $(CeS)_{1.5}TaS_2$, $CeTaS_3$, *Acta Cryst*. *C* **1991**, *47*, 924–930.
[13] M. Nath, C. N. R. Rao, New Metal Disulfide Nanotubes, *J*. *Am*. *Chem*. *Soc*. **2001**, *123*, 4841–4842.
[14] M. Nath, C. N. R. Rao, Nanotubes of the disulfides of groups 4 and 5 metals, *Pure Appl*. *Chem*. **2002**, *74*, 1545–1552.
[15] M. Nath, C. N. R. Rao, Nanotubes of Group 4 Metal Disulfides, *Angew*. *Chem*. *Int*. *Ed*. **2002**, *41*, 3451–3454.
[16] L. E. Conroy, K. R. Pisharody, The preparation and properties of single crystals of the 1*S* and 2*S* polymorphs of tantalum disulfide, *J*. *Solid State Chem*. **1972**, *4*, 345–350.
[17] G. Seifert, H. Terrones, M. Terrrones, S. Jungnickel, T. Frauenheim, Structure and Electronic Properties of MoS_2, *Phys*. *Rev*. *Lett*. **2000**, *85*, 146–149.
[18] G. Seifert, H. Terrones, M. Terrrones, T. Frauenheim, Novel NbS_2 metallic nanotubes, *Solid State Commun*. **2000**, *115*, 635–638.
[19] G. Seifert, T. Köhler, R. Tenne, Stability of Metal Chalcogenide Nanotubes, *J*. *Phys*. *Chem*. *B* **2002**, *106*, 2497–2501.
[20] V. V. Ivanovskaya, A. N. Enyashin, N. I. Medvedeva, A. L. Ivanovskii, Electronic properties of superconducting $NbSe_2$ nanotubes, *Phys*. *Stat*. *Sol*. *B* **2003**, *238*, R1–R4.
[21] V. V. Ivanovskaya, A. N. Enyashin, N. I. Medvedeva, Yu. N. Makurin, and A. L. Ivanovskii, Computational Studies of Electronic Properties of ZrS_2 Nanotubes, *Internet Electron. J. Mol. Des.* **2003**, *2*, 499–510, http://www.biochempress.com.
[22] V. V. Ivanovskaya, G. Seifert, Tubular structures of titanium disulfide TiS_2, *Solid State Commun*. **2004**, *130*, 175–180.
[23] M. Methfessel, M. Scheffler, Full–potential LMTO calculations for atomic relaxations at semiconductor–semiconductor interfaces, *Physica B* **1991**, *172*, 175–183.
[24] J. P. Perdew, Y. Wang, Accurate and simple analytic representation of the electron–gas correlation energy, *Phys*. *Rev*. *B* **1992**, *45*, 13244–13249.
[25] S. Y. Savrasov, Linear–response theory and lattice dynamics: A muffin–tin–orbital approach, *Phys*. *Rev*. *B* **1996**, *54*, 16470–16486.
[26] H. Whangbo, R. Hoffmann, The band structure of the tetracyanoplatinate chain, *J*. *Am*. *Chem*. *Soc*. **1978**, *100*, 6093–6098.
[27] Z. Y. Wu, G. Ouvrard, P. Moreau, C. R. Natoli, Interpretation of preedge features in the Ti and S K–edge x–ray–absorption near–edge spectrain the layered disulfides TiS_2 and TaS_2, *Phys*. *Rev*. *B* **1997**, *55*, 9508–9513.
[28] M. Nath, S. Kar, A. K. Raychaudhuri, C. N. R. Rao, Superconducting $NbSe_2$ nanostructures, *Chem*. *Phys*. *Lett*. **2003**, *368*, 690–695.